Robust Cylinder Estimation in Point Clouds from Pairwise Axes Similarities

Mara Pistellato, Filippo Bergamasco, Andrea Albarelli and Andrea Torsello
DAIS, Ca'Foscari University of Venice, Via Torino 155, Venice, Italy

Keywords: Cylinder Fitting, Point Clouds, Industrial Reconstruction, Game Theory, Dual-quaternions, Model Fitting.

Abstract: The ubiquitous presence of cylindrical shapes in both natural and man-made environments makes their automated extraction a pivotal task for a broad range of applications such as robot manipulation, reverse engineering and automated industrial inspection. Albeit conceptually simple, the task of fitting cylinders from 3D data can quickly become challenging if performed "in-the-wild", when no prior is given to the number of primitives to find or when the point cloud is noisy and not oriented. In this paper we introduce a new robust approach to iteratively extract cylindrical primitives from a 3D point cloud by exploiting mutual consensus of different cylinder candidates. First, a set of possible axes is generated by slicing the point cloud with multiple random planes. Then, a game-theoretic inlier selection process is performed to extract a subset of axes maximizing the fitness against a payoff function based on the shortest geodesic path in SE(3) between pairs of corresponding 3D lines. Finally, the probability distribution resulting from the previous selection step is used to weight the input candidates and robustly obtain the final cylinder coefficients. Compared to other methods, our approach does not require point normals, offers superior resilience to noise and does not depend on delicate tuning of multiple parameters.

1 INTRODUCTION

Cylinders, and other quadrics in general, represent more than 85% of the objects that can be found in industrial and human made scenes (Hakala et al., 1980). Their automated segmentation and extraction is an important task in a broad range of applications, ranging from industrial automation (Rahayem and Kjellander, 2011) to natural landscapes analysis (Pfeifer et al., 2004). Popular applications in this context include robot manipulation (Specian et al., 2018), automated pipe-run reconstruction (Qiu et al., 2014), intake measurements (Bergamasco et al., 2012) and Geometric Reverse Engineering (Lukács et al., 1997). All the aforementioned applications operate on 3D spatial information that must be acquired from a scene. Notwithstanding the recent advances in 3D reconstruction techniques, the availability of a high-quality oriented point cloud is not always affordable in practice. For example, shiny metal surfaces still represent a challenge situation that may lead to incomplete or noisy 3D surfaces (Amir and Thörnberg, 2017). For this reason, any robust quadrics fitting technique must rely to some sort of outlier detection to be used in practice. In the specific case of cylinders, various methods have been proposed in the literature that operate directly on 3D point clouds. As a general taxonomy, we can distinguish between *fitting algorithms* and *extraction algorithms*. The formers require pre-segmented point clouds, where each point must be associated a-priori to each different cylindrical object. They are typically based on a non-linear least-squares minimization of the point distances to the cylindrical surface (Lukács et al., 1998). However, given the well known sensitivity of least squares to outliers, they tend to suffer to the poor quality of such mandatory cylinder segmentation. Methods belonging to the latter category use statistically robust techniques to extract cylinder shapes out of a noisy point cloud. They are usually less accurate than the former but exhibit a clear advantage when point data include clutter, spurious points and incomplete areas. This category can be further split among methods that require oriented point clouds (where a normal vector is associated to each 3D point) and the ones that only rely on the reciprocal position of points. The former makes heavy use of surface normals to reduce the search space of cylinder parameters by means of sample consensus techniques (Torr and Zisserman, 2000) or specially designed voting spaces (Rabbani and den

Heuvel, 2005). Unfortunately, reliable surface normal is in general more difficult to obtain than the point cloud itself. Hence, the quality of normal vectors directly affects the reliability of the cylinder extraction technique. If the point cloud is not oriented, parameter search space quickly grows to a dimensionality where voting or consensus techniques become less effective in practice. Recently, (Rahayem et al., 2012) proposed a method that just requires point clouds (acquired from laser scanner) to extract and fit cylindrical shapes. Albeit being robust to noisy data, it can operate on a scene composed by a single cylinder at a time. In this paper we propose a novel cylinder extraction technique also belonging to this latter category. We build our method on the same basic idea of (Rahayem et al., 2012) expanding the technique to work with a simultaneous presence of multiple cylinders and extreme noise conditions. Compared to existing methods, our approach offers three main advantages. First, it is almost parameter free. There are no requirements about prior knowledge on the geometry of the point cloud or the characteristics of the cylinders involved in the scene. This is mostly due to the game-theoretical process that is able to reliably perform inlier selection based on mutual consensus of multiple candidates. Second, it offers accurate results since multiple hypotheses are averaged on the basis of their relative fitting score to a common cylindrical model. Third, it can work reliably even if most of the cylindrical shape is not available due to self-occlusion. In practice, primitives can be fit out from a single scanner range image. An extensive evaluation presented in Section 3 demonstrates all these features on both synthetic and real-world cases.

2 THE PROPOSED METHOD

We restrict our application to cylindrical shapes defined by the locus of points lying at a distance r to a 3D line in space, called axis[1].

We over-parametrize a cylinder ζ with the triplet $(p,\vec{v},r)$ where $p \in \mathbb{R}^3$ and $\vec{v} \in \mathbb{R}^3$ define axis point and direction respectively. We pose the additional constraints of $\|v\| = 1$ and $\langle p,\vec{v}\rangle = 0$ resulting in only 5 degrees of freedom out of the 7 parameters used for the parametrization. The intersection between ζ and a plane P (whose normal $\vec{n}$ is not orthogonal with $\vec{v}$) results in an ellipse E with the following properties (See Fig. 1, Left): (i) the minor semi-axis b is equal to the cylinder's radius r; (ii) the ellipse center c lies on the cylinder axis; (iii) The ratio between the semi-major axes a and b is related to the angle α between $\vec{v}$ and $\vec{n}$ according to the formula $\cos\alpha = \frac{b}{a}$.

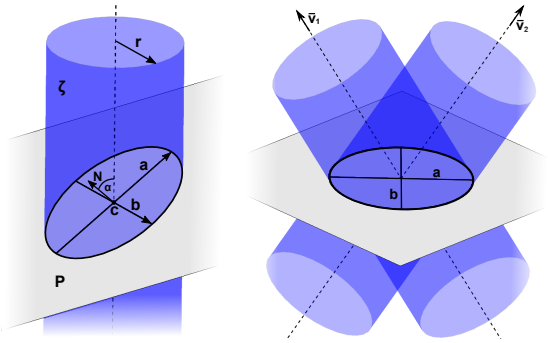

Figure 1: Left: plane-cylinder intersection. Right: two possible cylinders deriving from an ellipse in 3D space.

These properties can be used to extract cylinders from planar slices of a 3D point cloud. For simplicity, let's assume to have acquired a scene containing one single cylindrical shape and many other points resulting from other objects or noise. If 3D data is sufficiently dense, a subset S of points can be extracted comprising all the samples lying close to a plane P, that we suppose not being parallel to the cylinder axis. According to what said before, some of the points will lie on the ellipse generated by the cylinder in the scene, some others will be distributed with no particular pattern (ie. they are outliers with respect to the elliptical shape). Therefore, any sufficiently robust fitting operation that extracts the elliptical shape E out of S will give clues on the unknown cylinder present in the scene.

In particular, the minor axis of E will define the radius of the cylinder and the center c the position of the axis. Similarly to what happens with camera poses (Bergamasco et al., 2014), the ratio between a and b determines the direction $\vec{v}$ up to two equally-possible configurations (See Fig.1, Right). Due to this intrinsic ambiguity, at least two plane slices are needed to fully recover the coefficients of a cylinder.

In their paper, (Rahayem et al., 2012) propose to use multiple slices to collect the centers $(c_1 \dots c_n)$ and minor axes $(b_1 \dots b_n)$ of each fitted ellipses. This way, the cylinder radius is recovered averaging each $b_1 \dots b_n$ and the axis $(p,\vec{v})$ by fitting a 3D line to $c_1 \dots c_n$ in a least-squares sense. The approach has three drawbacks. First, it totally discards information given by each ellipse regarding the possible orientation of cylinder axis (due to the mentioned ambiguity). Second, it can only handle a single cylinder in the data. Third, can badly suffer from possible wrong estimations since all the values are averaged without weighting their reliability. This aspect is partially rel-

[1]This implies that the considered cylinders extends infinitely along their axes

evant though since the following non-linear optimization may still be able to recover the correct shape.

Our approach follows a similar strategy. We slice the scene with n different random planes. From the 2D scattered point set obtained in each section $i = 1 \dots n$, we robustly extract all the $j = 1 \dots N_i$ possible ellipses using RANSAC and the ellipse model estimation method described in (Halır and Flusser, 1998). When considered in 3D space, each extracted ellipse $E_{i,j}$ is defined by its major and minor semi-axes vectors $\vec{a}_{i,j} \in \mathbb{R}^3$ and $\vec{b}_{i,j} \in \mathbb{R}^3$ and its center $c_{i,j} \in \mathbb{R}^3$. By construction, $\vec{a}_{i,j}$ and $\vec{b}_{i,j}$ are both defined up to a sign and orthogonal to the normal $\vec{n}_i$ of the i^{th} plane.

From each $E_{i,j}$, we compute the two possible cylinder candidates as the tuples $(r, c, \vec{v}^1)_{i,j}$ and $(r, c, \vec{v}^2)_{i,j}$, where:

$$\begin{aligned} r &= \|\vec{b_{i,j}}\| \\ c &= c_{i,j} \\ \vec{v}^1 &= \mathbf{R}\,\vec{n}_i \\ \vec{v}^2 &= \mathbf{R}^T\vec{n}_i \\ \mathbf{R} &= \mathbf{I} + \sqrt{1 - \frac{\|\vec{b_{i,j}}\|^2}{\|\vec{a_{i,j}}\|^2}} \left[\frac{\vec{b_{i,j}}}{\|\vec{b_{i,j}}\|}\right]_\times + \\ &\quad + (1 - \frac{\|\vec{b_{i,j}}\|}{\|\vec{a_{i,j}}\|}) \left[\frac{\vec{b_{i,j}}}{\|\vec{b_{i,j}}\|}\right]^2_\times . \end{aligned} \tag{1}$$

In the tuples, r and c denote the cylinder radius and axis point shared by the two candidates. [2]. Conversely, $\vec{v}_1$ and $\vec{v}_2$ are the two possible axis orientations obtained by rotating the plane normal $\vec{n}_i$ around the minor-axis of the ellipse $E_{i,j}$ with an angle of $\pm \arccos \frac{\|\vec{b_{i,j}}\|}{\|\vec{a_{i,j}}\|}$.

2.1 Cylinder Similarity Function

Extracting the most probable cylinder out of all the generated tuples can be seen as a clustering problem. Indeed, we aim to extract the largest group of candidates that are all consistent with respect to one specific cylinder model in the scene. To do so, we must first define a similarity function between any two candidates to measure their consistency against a common model. The non-trivial aspect is that, a part from the relative radii, to have a well-defined function both the combined axes positions and orientations must be considered .

We start by defining a distance between two 3D axes in space. Let $l_1 = (c_1, \vec{v}_1)$ and $l_2 = (c_2, \vec{v}_2)$ be two 3D lines defined respectively by a point c and a unitary-norm vector $\vec{v}$. Following (Bergamasco et al., 2015) , we construct a rigid motion $(\bar{\mathbf{R}}, \bar{T})$ mapping line l_1 to l_2 or, more formally, the roto-translation such that $\forall p \in l_1, \exists\, k \in \mathbb{R}.\, \bar{\mathbf{R}}p + \bar{T} = c_2 + k\vec{v}_2$. Among all the possible motions, we can easily express the one exhibiting the shortest translation length and smaller rotation angle taking advantage of the kinematic notion of a screw. That is, every rigid-motion can be modeled as a rotation with a certain angle about an axis (not necessarily passing through the origin) followed by a translation along that axis (Chen, 1991). In our case, let $m_1 = c_1 + t_1\vec{v}_1$ (for some scalar t_1) be the point of line l_1 closest to the line l_2. Similarly, let $m_2 = c_2 + t_2\vec{v}_2$ be the point of l_2 closest to line l_1. By construction, the vector $T = m_2 - m_1$ is orthogonal to both l_1 and l_2 and its length is the minimum distance between all the points of the two lines. This implies that T has the same direction (but possibly different length and orientation) of the vector $\vec{v}_\perp = \vec{v}_1 \times \vec{v}_2$. So, the rotation with angle $\beta = \arcsin(\|\vec{v}_\perp\|)$ around the axis defined by point m_1 and vector $\vec{s} = \vec{v}_\perp / \|\vec{v}_\perp\|$ will let l_1 be parallel to l_2. Since m_1 lies on the rotation axis, its position will not change after the transformation, hence the distance between the two lines will remain equal to $\|T\|$. Trivially, a final translation along T will let l_1 coincide with l_2.

Such modelling is convenient because the parameters of the screw motion can be related to the scalar and vector part of a unit dual quaternion $\hat{\mathbf{q}}$ (Eq.2):

$$\begin{aligned} \hat{\mathbf{q}} &= \cos\frac{\hat{\theta}}{2} + \hat{\mathbf{s}}\sin\frac{\hat{\theta}}{2} \\ \hat{\theta} &= 2\beta + \varepsilon 2\|T\| \\ \hat{\mathbf{s}} &= \mathbf{i}\vec{s} + \varepsilon\mathbf{i}(m_1 \times \vec{s}) \end{aligned} \tag{2}$$

In the expression, $\mathbf{i} = (i, j, k)$ is the row vector of quaternions imaginary bases, $\hat{\mathbf{s}}$ is a dual quaternion (with zero scalar part) describing the rotation axis and $\hat{\theta}$ is the dual angle expressing the angle of rotation and the amount of translation.

The set of unit dual quaternions is a 6-dimensional manifold embedded an 8-dimensional Euclidean space (McCarthy, 1990) for which the corresponding log map can be defined in closed form as in (3)

$$log(\hat{\mathbf{q}}) = \hat{\mathbf{s}}\frac{\hat{\theta}}{2}. \tag{3}$$

The existence of such log map allow us to define a distance function between l_1 and l_2 induced by the length of the geodesic path in SE(3) from the origin (ie. the identity motion) to $\hat{\mathbf{q}}$:

$$d(l_1, l_2) = \min(\|\log(\hat{\mathbf{q}})\|, \|\log(-\hat{\mathbf{q}})\|) \tag{4}$$

[2] Matrix $\mathbf{R}$ is obtained by Rodrigues' formula. The symbol $[.]_\times$ denotes the skew-symmetric matrix of the cross-product.

Note that in (4) the minimum is necessary due to the *antipodal* property of dual quaternions (i.e. $\hat{\mathbf{q}}$ and $-\hat{\mathbf{q}}$ represent the same transformation but with two different trajectories). For more informations about dual numbers and dual quaternion algebra for geometric applications we suggest (Daniilidis, 1999; Kavan et al., 2008). With the defined distance between two cylinder axes, we can finally formulate a similarity function between two candidates $\xi_1 = (r_1, c_1, \vec{v}_1^k)_{i_1,j_1}$ and $\xi_2 = (r_2, c_2, \vec{v}_2^h)_{i_2,j_2}$ as:

$$\pi(\xi_1,\xi_2) = \begin{cases} 1 & \text{if } \xi_1 = \xi_2 \\ e^{-\frac{d\left((c_1,v_1),(c_2,v_2)\right)}{\lambda}} & \text{if } \quad i_1 \neq i_2 \ \wedge \\ & Ad(\xi_1,\xi_2) < r_1 + r_2 \\ 0 & \text{otherwise} \end{cases} \tag{5}$$

where λ is a free parameter[3] and $Ad(\xi_1,\xi_2)$ is the minimum distance ($\|T\|$) between the two candidate axes (c_1,v_1) and (c_2,v_2) as defined previously. Eq.(5) is simple if we reason in terms of compatibility between candidates. The function assumes values between 0 (not compatible with the same cylindrical model) and 1 (fully compatible): any candidate has maximum similarity with itself and 0 similarity with any other candidate either generated by the same plane or with its axis further than the sum of the respective radii. The former may happen in two cases: (i) the candidate results from a distinct coplanar ellipse or (ii) has been generated by the same ellipse but with different $\vec{v}$. In the final case of "close" candidates from different planes, the similarity is made inversely proportional to the axis distance defined in (4) thanks to the negative exponential with factor λ.

2.2 The Inlier Selection Process

We cast the selection of a subset of candidates in the context of Evolutionary Game Theory (Weibull, 1995). In such scenario we have that pairs of individuals, belonging to a certain population, play a game one versus the other on the basis of pre-programmed strategies. A selection process brings some individuals matching well together to thrive, while driving the "unfitting" ones to extinction.

In our specific case, all the $M = \sum_{i=1}^{n} N_i$ cylinder candidates $\xi_1 \dots \xi_M$ are the individuals that we call *hypotheses*. We express how well two hypotheses play together by defining a fitness through the *payoff-function*, formulated as in (5) that can be conveniently represented as an $M \times M$ symmetric matrix Π in which an element at row i and column j is equal to $\pi(\xi_i,\xi_j)$. We consider a discrete probability distribution $\mathbf{x} = (x_1, x_2, \dots, x_M)$ over the set of hypotheses. The problem of finding a coherent set of candidates can be described formally in finding a particular distribution $\mathbf{x} \in \Delta^n$ maximizing the average payoff $\mathbf{x}^T \Pi \mathbf{x}$. One possible solution to the problem employs an evolutionary process starting from a uniform distribution $\mathbf{x}^{(0)}$ and evolving through the common *discrete-time replicator dynamic* (Taylor and JONKER, 1978)

$$x_i^{(t+1)} = x_i^{(t)} \frac{(\Pi \mathbf{x}^{(t)})_i}{\mathbf{x}^{(t)^T} \Pi \mathbf{x}^{(t)}} \tag{6}$$

Equation (6) belongs to a class of evolutionary dynamics called *Payoff-Monotonic Dynamics* that are guaranteed to converge to a solution $\hat{\mathbf{x}}$ in which the set of hypotheses with associated probability greater than 0 (namely the *support* of a population) cannot include any strategy with mutual payoff equal to 0. In other words, the candidates with associated non-zero probability in $\hat{\mathbf{x}}$ will be the ones generated from different planes and with the distance between the two axes greater than the sum of the two radii. After the inlier selection process, the final cylinder axis is computed by fitting a line through the centres of the winning candidates in a least-squares sense.

2.3 Extracting Multiple Cylinders

To extract multiple cylinders, the inlier selection is simply repeated by ensuring that the winning candidates resulting from the previous extraction cannot be selected anymore. Specifically, after the extraction of each cylinder, we modify the payoff matrix Π according to the current population support.

Let $k_1, k_2, \dots k_h$ be the set of indices of non-zero elements of $\hat{\mathbf{x}}$ (ie. $\hat{x}_K = 0 \ \ \forall K \in k_1 \dots k_h$). Π is modified so that all the rows and columns at indices $k_1 \dots k_h$ are set to zero. After that, the initial population $\mathbf{x}^0$ is reset to the uniform distribution and the inlier selection process (6) is run again until convergence. Since we are using a payoff-monotonic dynamic, all the previous candidates indexed by $k_1 \dots k_h$ cannot be included in the next set of winning candidates. Such process is repeated until all the cylinders are extracted from the scene.

3 EXPERIMENTAL EVALUATION

To assess the effectiveness of our approach, we devised a set of tests in synthetical and real-world environments. The former allows us to control several factors (noise, outliers, data sampling) and it is designed

[3] In all our tests we fixed $\lambda = 5$.

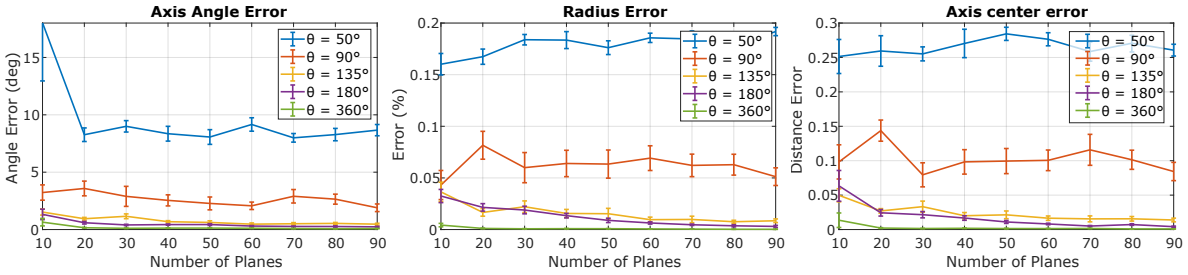

Figure 2: Angle, radius and center errors varying the number of randomly generated planes. Each curve denotes a different cylinder surface coverage (corresponding to the angle θ).

to capture the potentials of our approach. Since our method is addressed to real-world applications, a set of qualitative experiments performed on real scans will be presented as well.

Synthetic Setup. We generated a cylinder centered at origin, aligned to the z-axis and with unitary radius. All its points were perturbed with a zero-mean additive Gaussian noise of standard deviation σ. Additionally, some outlier points were perturbed with a salt and pepper noise, with a different standard deviation denoted as σ_o (with $\sigma_o > \sigma$). The amount of outliers is controlled by a parameter p, that is the probability for a point to be an outlier. Since most of the time range data does not cover all the cylinder's surface, we also introduced a parameter θ, that is the angle underlying the covered cylinder's surface. In the case $\theta = 360^\circ$, the object is complete. For each experiment we measured the fitting precision through three different quantities, namely the radius relative error (in % with respect to the actual value), the axis rotation and translation errors.

3.1 Sensitivity Analysis

As discussed, the number of slicing planes is the only parameter required by our method. The number of planes affects the robustness of the proposed algorithm, and should be adjusted depending on the features of the acquired scene. For this reason we started by analysing how important is this parameter for the stability of our approach. Specifically, we tested our algorithm varying the number of random planes (ranging from 10 to 90) and their inclination with respect to the real cylinder's axis.

In the first experiment, we tested the goodness of the cylinder fitting for different surface coverages (determined by the angle θ) for a synthetically generated a cylinder with $\sigma = 0.005$ and $\sigma_o = 0.01$ with $p = 0.1$. Figure 2 shows the results in three plots that are angle, radius and translation error. Each configuration was tested 10 times and the error bars display the standard error of the mean. As expected, plots show an improved accuracy as the angle θ increases, due to a better ellipse fitting. In particular, for the angles higher than 135° we can observe minor changes in terms of precision, since the curves shrink in the lower part of each plot. The curves exhibit the same general behaviour, that is an overall improvement and stability as the number of slicing planes increases. Despite this, we noticed that the number of planes is not as critical as one could expect: in cases or medium levels of noise, 30 to 50 planes could be a suitable number to obtain a reasonably good result. Of course, if the scene to be processed contains more than one primitive to be extracted, the number of planes should be kept high to capture all the relevant elements.

3.2 Comparisons

In this section we compare the performances of the proposed technique with two different methods. We employed the previously described synthetic setup, working with a single cylinder scenario. This allows us to separate the precision of the fitting algorithm from the primitive extraction ability. We compared our technique with (Rahayem et al., 2012) and (Torr and Zisserman, 2000). The first computes the cylinder's axis fitting a line through the centers of the ellipses, and computes the radius as the mean value of all the radii, then refines the fitting through a non-linear optimization. In the following comparisons we used the same ellipses as input. The second approach consists in a sample consensus technique which exploits points normals to compute the best cylinder estimate in a point cloud. We run this algorithm setting the maximum inlier distance at 0.03, with 5000 maximum iterations.

In the first experiment we tested the reconstruction ability in presence of escalating Gaussian noise levels. We fixed the outlier parameters $\sigma_o = 0.04$ and $p = 0.3$, while increasing the standard deviation of the additive noise from 0.001 to 0.05. For each experiment we extracted 20 random planes and repeated each test 20 times. Figure 3 shows the resulting error plots, where the bars denote the standard error val-

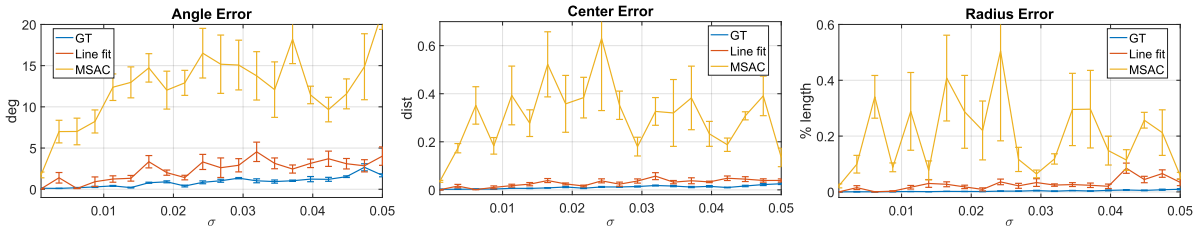

Figure 3: Angle, center and radius error means increasing the standard deviation of additive, zero-mean Gaussian noise. We tested three different cylinder fitting technique, each one denoted by a curve.

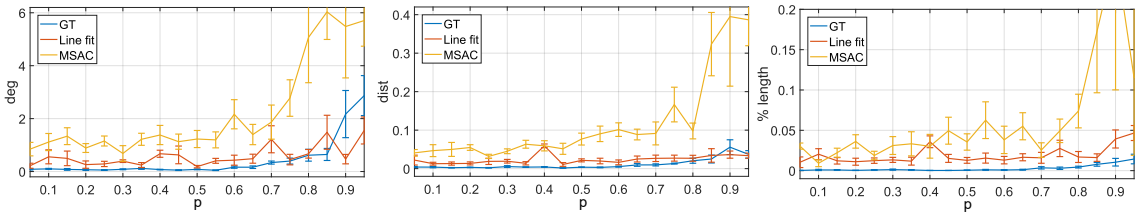

Figure 4: Angle, center and radius error means varying the salt and pepper noise parameters. We increased the outlier probability p and keep $\sigma_o = 0.1$;. Each curve denotes a different cylinder fitting technique.

ues. In the case of center dislocation and radius errors, our algorithm and the line fitting method offer similar results. Nevertheless, our approach is able to provide a more stable and accurate result. In the case of axis rotation error, our technique results in a more precise assessment, thanks to the intrinsic outlier selection performed by the game theoretical approach.

The second group of experiments is designed to compare the performances of the three methods with different amounts of outliers. Figure 4 shows the behaviour of the techniques varying the outliers' frequency: we fixed $\sigma_o = 0.1$ and increased the value of p. In all tests we set $\sigma = 0.001$ and extracted the ellipses from 20 random planes. All tests were repeated 10 times for each configuration. The proposed approach outperforms the other methods, in particular it offered a high level of robustness when the outlier component is significant.

Finally, we compared the accuracy achievable when the scene is partially occluded. In the last comparison experiment (Fig.5) we performed the fitting for different values of θ, which is the angle that expresses the amount of covered cylinder's surface. The MSAC approach was not accounted since its error values were too high to be included in the visualisation. We set the additive Gaussian noise standard deviation $\sigma = 0.005$; while the outlier parameters were $\sigma_o = 0.01$ and $p = 0.1$. We also increased the number of random planes to 40 (with any inclination angle) to have a more stable result. The performances of our approach and the line fitting method are similar looking at the recovered center dislocation and radius relative error (center and right plots); in particular the line fitting algorithm performed slightly better with angles smaller than 90°. As the other experiments had already pointed out, the critical factor in cylinder fitting is the correct axis angle. The leftmost plot of Figure 5 shows the improvements of our approach with respect to the other method, increasing the axis precision up to 4 degrees.

In general the proposed game theoretical algorithm provides more stable results if compared to other techniques. It sometimes offers slightly better results with respect to the fitting line technique, but the accuracy in many cases is superior, especially with many outliers. Also, the axes angle is a critical element to be recovered, and our algorithm ensures the best candidate selection.

3.3 Real-world Experiments

We employed actual scans to test the capabilities of our approach in real-world applications. We used the point cloud dataset presented in (Calli et al., 2017), that contains scans of the Yale-CMU-Berkeley Object and Model Set (Calli et al., 2015). The dataset contains coloured point data of several objects with no surface normals. We selected a subset of them to create a number of scenes in which some cylinders are to be extracted. Moreover, we aim to evaluate the goodness of our algorithm in presence of multiple cylindrical shapes of unknown location.

The first test was designed to measure the repeatability of the extraction algorithm, along with its capability in locating primitives given real-world data. We generated a scene containing two instances of the object *"tomato soup"* (radius = 33 mm, height = 101 mm) arranged at a known random translation.. The corresponding point cloud contains 373,205 vertices

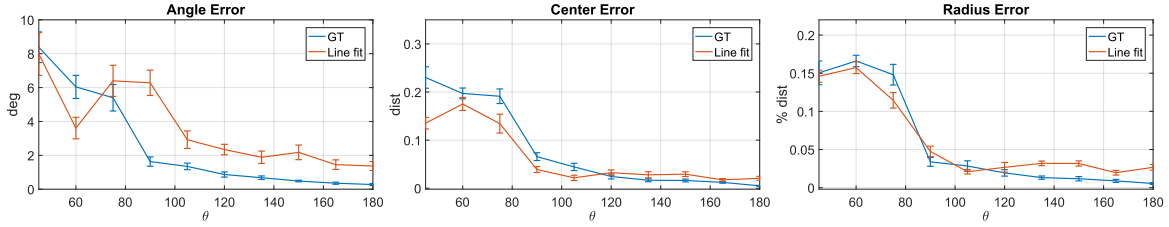

Figure 5: Angle, center and radius error means increasing the cylinder coverage angle θ.

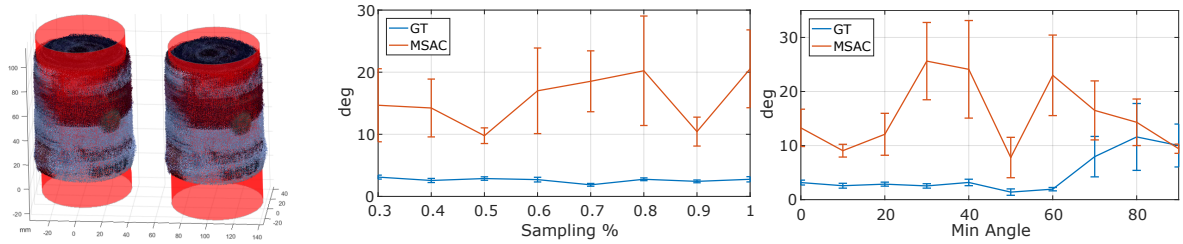

Figure 6: Left: an example of the generated scene with two scans of tomato soup object. In red, the cylinders fitted by our method. Center and right: relative angle means of the two fitted axes from the scene. The bars represent the standard error.

and appears quite thick, with no outliers. Figure 6 (left) shows an example of generated scene, together with the cylinders extracted by our method (in red). We exploited this setting to compare our algorithm with MSAC approach. The line fitting method (Rahayem and Kjellander, 2011) was excluded because it can not be applied in a scene for multiple cylinder extraction. To extract multiple primitives with MSAC, we iteratively removed the points belonging to a cylinder if their distance from the fitted axis is between $\pm 5\%$ of the radius. The surface normals (used in MSAC) have been computed by fitting a plane on 80 neighbour points that we empirically determined giving good results. The ellipses extraction from the slicing planes is performed just once, then the game theoretical approach selects a group of inliers using a different payoff matrix, as explained in 2.3. Since the exact center and axes of the objects is unknown, we evaluated the repeatability and accuracy of the extractions measuring the relative angle between the couple of fitted axes. Ideally, these values should be as closest to zero as possible. In the central plot of Figure 6 we show the relative angle between the pairs of fitted axes, varying the proportion of randomly sampled data from the original point cloud. We run our algorithm generating 40 planes and MSAC setting 3000 iterations and minimum inlier distance equal to 2mm. In the rightmost plot of Figure 6 we computed the same quantity filtering out the points for which the angle between their normal and a predefined direction is above a threshold (specified on the x-axis). In this way we simulated an incomplete acquisition, as we had a range-map (note that min angle = 0 corresponds to the whole point cloud). We used $(0, 1, 0)$ as "observing" direction and run the tests by randomly sampling the 80% of the points. We used 50 planes and increased the number of MSAC iterations to 5000. Each test was performed 20 times. In all the experiments our algorithm gave an angle between 2 and 5 degrees, except for the final part of the rightmost plot, where the error reaches 10 degrees. In all cases, MSAC approach exhibited an unstable behaviour and a higher standard error, likely due to an inaccurate normal estimation. We additionally tested the extraction algorithm "in the wild", generating random scenes with various features and using 60 slicing planes. In Figure 7 a selection of qualitative results is shown. In the leftmost example we used objects of different radius and height: *"tomato soup"* (radius 33 mm), *"Master Chef"* (radius 51 mm) and *"c cup"* (radius 32.5 mm). Each computed radius is displayed next to the corresponding cylinder. The central picture shows a configuration of nine *"tomato soup"* items, for which we run 9 times the inlier selection process to extract all the cylinders. Finally, the rightmost image shows an example of a generic scene with various items. Such results show the capability of our technique to correctly extract cylinder primitives in an heterogeneous scene, intrinsically excluding all non-cylindrical 3d data.

4 CONCLUSIONS

We proposed a novel technique to extract multiple cylindrical objects from generic point clouds. The game theoretic process combined with a specially designed payoff-function among cylinder candidates al-

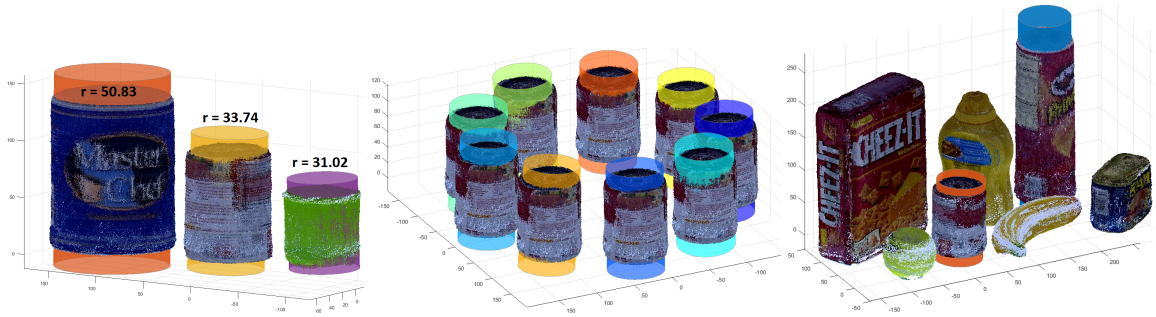

Figure 7: Qualitative examples obtained in different kinds of scenes, generated using real scans data.

low the method to be general enough to be used without prior knowledge of the scene. Our approach exhibits a high robustness with respect to outliers, that makes it perfect to be applied in scenarios where a noisy point cloud is acquired without normal vectors. Qualitative experiments show that the proposed extraction method offers high flexibility in very heterogeneous and complex scenes.

REFERENCES

Amir, Y. M. and Thörnberg, B. (2017). High precision laser scanning of metallic surfaces.

Bergamasco, F., Albarelli, A., Cosmo, L., Torsello, A., Rodolà, E., and Cremers, D. (2015). Adopting an unconstrained ray model in light-field cameras for 3d shape reconstruction. volume 07-12-June-2015, pages 3003–3012. cited By 6.

Bergamasco, F., Cosmo, L., Albarelli, A., and Torsello, A. (2012). A robust multi-camera 3d ellipse fitting for contactless measurements. pages 168–175.

Bergamasco, F., Cosmo, L., Albarelli, A., and Torsello, A. (2014). Camera calibration from coplanar circles. pages 2137–2142.

Calli, B., Singh, A., Bruce, J., Walsman, A., Konolige, K., Srinivasa, S., Abbeel, P., and Dollar, A. M. (2017). Yale-cmu-berkeley dataset for robotic manipulation research. *The International Journal of Robotics Research*, 36(3):261–268.

Calli, B., Singh, A., Walsman, A., Srinivasa, S., Abbeel, P., and Dollar, A. M. (2015). The ycb object and model set: Towards common benchmarks for manipulation research. In *Advanced Robotics (ICAR), 2015 International Conference on*, pages 510–517. IEEE.

Chen, H. H. (1991). A screw motion approach to uniqueness analysis of head-eye geometry. In *Proceedings. CVPR 1991*, pages 145–151.

Daniilidis, K. (1999). Hand-eye calibration using dual quaternions. *The International Journal of Robotics Research*, 18(3):286–298.

Hakala, D., Hillyard, R., and Malraison, P. J. (1980). Natural quadrics in mechanical design. In *CAD/CAM VIII part of Autofact West Anaheim*, California.

Halır, R. and Flusser, J. (1998). Numerically stable direct least squares fitting of ellipses. In *Proc. 6th International Conference in Central Europe on Computer Graphics and Visualization. WSCG*, volume 98, pages 125–132. Citeseer.

Kavan, L., Collins, S., Žára, J., and O'Sullivan, C. (2008). Geometric skinning with approximate dual quaternion blending. *ACM Trans. Graph.*, 27(4):105:1–105:23.

Lukács, G., Marshall, A. D., and Martin, R. R. (1997). Geometric least-squares fitting of spheres , cylinders , cones and tori.

Lukács, G., Martin, R., and Marshall, D. (1998). Faithful least-squares fitting of spheres, cylinders, cones and tori for reliable segmentation. In *Computer Vision - ECCV'98*, pages 671–686.

McCarthy, J. M. (1990). *Introduction to Theoretical Kinematics*. MIT Press, Cambridge, MA, USA.

Pfeifer, N., Gorte, B., and Winterhalder, D. (2004). Automatic reconstruction of single trees from terrestrial laser scanner data.

Qiu, R., Zhou, Q.-Y., and Neumann, U. (2014). Pipe-run extraction and reconstruction from point clouds. In *Computer Vision – ECCV 2014*, pages 17–30.

Rabbani, T. and den Heuvel, F. A. V. (2005). Efficient hough transform for automatic detection of cylinders in point clouds.

Rahayem, M., Werghi, N., and Kjellander, J. (2012). Best ellipse and cylinder parameters estimation from laser profile scan sections. *Optics and Lasers in Engineering*, 50(9):1242 – 1259.

Rahayem, M. R. and Kjellander, J. A. P. (2011). Quadric segmentation and fitting of data captured by a laser profile scanner mounted on an industrial robot. *The International Journal of Advanced Manufacturing Technology*, 52(1):155–169.

Specian, A., Mucchiani, C., Yim, M., and Seo, J. (2018). Robotic edge-rolling manipulation: A grasp planning approach. *IEEE Robotics and Automation Letters*, 3(4):3137–3144.

Taylor, P. D. and JONKER, L. B. (1978). Evolutionarily stable strategies and game dynamics.

Torr, P. H. S. and Zisserman, A. (2000). MLESAC: A new robust estimator with application to estimating image geometry. *CVIU*, 78:138–156.

Weibull, J. (1995). *Evolutionary game theory*. MIT Press, Cambridge, Mass. [u.a.].